

# Natural Convection of Water-Based CuO Nanofluids in a Cylindrical Enclosure

Baha Tulu Tanju and Kamil Kahveci

**Abstract**—Buoyancy driven heat transfer of nanofluids in a cylindrical enclosure used as a control unit in the subsea hydrocarbon injection wells is investigated in this study. The governing equations obtained with the Boussinesq approximation are solved using Comsol Multiphysics finite element analysis and simulation software. The base fluid is water and CuO is used as nanoparticles. Solution is obtained for nanoparticle solid volume fraction of 8% and for Rayleigh number in the range of  $10^5$ - $10^7$ . The results show that nanoparticle usage in the cylindrical electronic control unit has a significant effect on the flow and heat transfer.

**Keywords**—CuO, enclosure, nanofluid, natural convection

## I. INTRODUCTION

CONVENTIONAL heat transfer fluids have low thermal conductivities. This is the main drawback in enhancing the performance and the compactness of many engineering devices. Therefore, there is a strong need for advanced heat transfer fluids with substantially higher thermal conductivities. The way to meet this need is to use solid particles within a base fluid. Micron-sized particles have been used in the past, but sedimentation and clogging were persistent problems in fluids with these particles. The introduction of nanofluids has eliminated these drawbacks. The term nanofluid is used to describe a solid and liquid mixture that consists of a base liquid and nanoparticles sized less than 100nm. Ceramic particles, pure metallic particles, and carbon nanotubes are all used as nanoparticles. The presence of the nanoparticles causes an anomalous increase in the effective thermal conductivity of the fluid. Eastman et al. [1] found that the effective thermal conductivity of ethylene glycol increases up to 40% for a nanofluid containing approximately 0.3 vol % Cu nanoparticles of mean diameter less than 10 nm. Choi et al. [2] produced nanotube-in-oil suspensions and measured their effective thermal conductivity. The measured thermal conductivity were found to be anomalously greater than theoretical predictions. Xuan and Li [3] made a theoretical study on the thermal conductivity of nanofluids. The hot-wire apparatus was used to measure the thermal conductivity of nanofluids with suspended copper nanoparticle powders. They found that for the water-copper nanoparticle suspension, the ratio of the thermal conductivity of the nanofluid to that of the

B. T. T. Author is with Mechanical Engineering Department, Trakya University, 22030 Edirne, Turkey (phone: 284-235-8230; fax: 284-235-8237; e-mail: bahatanju@yahoo.com).

K. K. Author is with Mechanical Engineering Department, Trakya University, 22030 Edirne, Turkey (phone: 284-235-8230; fax: 284-235-8237; e-mail: kamilk@trakya.edu.tr).

base liquid varies from 1.24 to 1.78 if the volume fraction of the ultrafine particles increases from 2.5% to 7.5%. Keblinski et al. [4] investigated four possible mechanisms for this anomalous increase: Brownian motion of the nanoparticles, molecular level layering of the liquid at the liquid-particle interface, the nature of heat transfer in the nanoparticles, and nanoparticle clustering. They also showed that the Brownian motion is a negligible contributor, and that liquid layering around the nanoparticles could cause rapid conduction.

The aim of this study is to investigate natural convection of water-based CuO nanofluids in a cylindrical enclosure used as a control unit in subsea hydrocarbon injection wells.

## II. ANALYSIS

The basic configuration used in the analysis is shown in Fig. 1. The cylindrical enclosure of height  $H=500$ mm and diameter  $D=700$ mm has two small cylinders of diameter  $d=285$ mm in it, which dissipates heat from their surfaces.

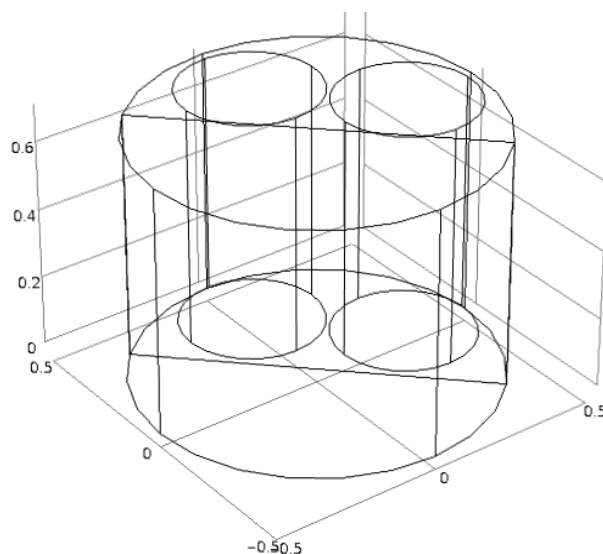


Fig. 1 Geometry and the coordinate system

In order to nondimensionalize the governing equations; the following dimensionless variables are used:

$$x = \frac{x^*}{D}, \quad y = \frac{y^*}{D}, \quad u = \frac{u^*}{\alpha_f}, \quad v = \frac{v^*}{\alpha_f}, \quad w = \frac{w^*}{\alpha_f},$$

$$P = \frac{D^2}{\rho_f \alpha_f^2} P^*, \quad T = \frac{T^* - T_C}{T_R - T_C} \quad (1)$$

where  $u^*$ ,  $v^*$ ,  $w^*$  are the dimensional velocity components in the  $x^*$ ,  $y^*$  and  $z^*$  directions, respectively,  $p^*$  is the dimensional pressure,  $T^*$  is the dimensional temperature,  $\rho$  is the density, and  $\alpha$  is the thermal diffusivity. The reference temperature  $T_R^*$  may be taken as  $T_R^* = T_C^* + Dq/k_f$  without losing the generality while keeping the dimensionless heat flux equal to one. The  $q$  is the heat flux from the surfaces of the inner cylinders.

The flow is assumed to be Newtonian, steady, and incompressible. The buoyancy effects are incorporated in the formulation by invoking the Boussinesq approximation. The viscous dissipation terms and the thermal radiation are assumed to be negligible. Despite the fact that a nanofluid is a two phase mixture, since the solid particles are of a very small size, they are easily fluidized and therefore can be considered to behave as a fluid. Therefore, it might be reasonable to treat a nanofluid as a single phase flow. The single phase approach assumes that the fluid phase and particles are in thermal equilibrium and move with the same velocity. This approach, which is simpler and requires less computational effort, is used in this study. With the foregoing assumptions, the dimensionless governing equations can be obtained as follows:

$$\frac{\partial u}{\partial x} + \frac{\partial v}{\partial y} + \frac{\partial w}{\partial z} = 0 \quad (2)$$

$$u \frac{\partial u}{\partial x} + v \frac{\partial u}{\partial y} + w \frac{\partial u}{\partial z} = -\frac{\rho_f}{\rho_{eff}} \frac{\partial P}{\partial x} + \frac{v_{eff}}{v_f} Pr \left( \frac{\partial^2 u}{\partial x^2} + \frac{\partial^2 u}{\partial y^2} + \frac{\partial^2 u}{\partial z^2} \right) \quad (3)$$

$$u \frac{\partial v}{\partial x} + v \frac{\partial v}{\partial y} + w \frac{\partial v}{\partial z} = -\frac{\rho_f}{\rho_{eff}} \frac{\partial P}{\partial y} + \frac{v_{eff}}{v_f} Pr \left( \frac{\partial^2 v}{\partial x^2} + \frac{\partial^2 v}{\partial y^2} + \frac{\partial^2 v}{\partial z^2} \right) \quad (4)$$

$$u \frac{\partial w}{\partial x} + v \frac{\partial w}{\partial y} + w \frac{\partial w}{\partial z} = -\frac{\rho_f}{\rho_{eff}} \frac{\partial P}{\partial z} + \frac{v_{eff}}{v_f} Pr \left( \frac{\partial^2 w}{\partial x^2} + \frac{\partial^2 w}{\partial y^2} + \frac{\partial^2 w}{\partial z^2} \right) + \frac{(\rho\beta_T)_{eff}}{\rho_{eff}\beta_{T,f}} RaPrT \quad (5)$$

$$u \frac{\partial T}{\partial x} + v \frac{\partial T}{\partial y} + w \frac{\partial T}{\partial z} = \frac{\alpha_{eff}}{\alpha_f} \left( \frac{\partial^2 T}{\partial x^2} + \frac{\partial^2 T}{\partial y^2} + \frac{\partial^2 T}{\partial z^2} \right) \quad (6)$$

where  $\nu$  is the kinematic viscosity,  $g$  is the gravitational acceleration and  $\beta_T$  is the coefficient of thermal expansion.  $\Delta T^*$  is the temperature difference. The Prandtl and Rayleigh numbers are defined as:

$$Pr = \frac{v_f}{\alpha_f}, \quad Ra = \frac{g\beta_{T,f}L^3\Delta T^*}{v_f\alpha_f} \quad (7)$$

Nondimensional governing equations are subjected to the following boundary conditions:

$$u|_s = 0, \quad v|_s = 0, \quad w|_s = 0 \quad \text{for all surfaces} \quad (8)$$

$$T|_s = 0 \quad \text{for outer cylinder} \quad (9)$$

$$\left. \frac{\partial T}{\partial n} \right|_s = -\frac{k_f}{k_{eff}} \quad \text{for inner cylinders} \quad (10)$$

$$T_{s,1} = T_{s,2}, \quad \frac{\partial T_{s,1}}{\partial n^*} = \frac{\partial T_{s,2}}{\partial n^*} \quad \text{for plate} \quad (11)$$

For the thermal conductivity of the nanofluid, the following approach proposed by Yu and Choi [5] was used:

$$\frac{k_{eff}}{k_f} = \frac{k_s + 2k_f + 2(k_s - k_f)(1 + \beta)^3\phi}{k_s + 2k_f - 2(k_s - k_f)(1 + \beta)^3\phi} \quad (12)$$

where  $\beta$  is the ratio of the nanolayer thickness to the original particle radius. Yu and Choi [5] compared their results for  $\beta=0.1$  with existing experimental results from previous studies and obtained reasonably good agreement.

Nanofluid viscosity is generally estimated using existing relations for a two-phased mixture. The following Brinkman model was used as the relation for the effective viscosity in this study.

$$\mu_{eff} = \frac{\mu_f}{(1 - \phi)^{2.5}} \quad (13)$$

Xuan and Li [6] experimentally measured the effective viscosity of a transformer oil-water nanofluid and a water-copper nanofluid within a temperature range of 20–50°C. Their experimental results showed reasonably good agreement with Brinkman's theory.

Other properties of nanofluid that are present in the governing equations can be defined by the following relations:

$$(\rho C_p)_{eff} = (1 - \phi)(\rho C_p)_f + \phi(\rho C_p)_s \quad (14)$$

$$(\rho\beta_T)_{eff} = (1 - \phi)(\rho\beta_T)_f + \phi(\rho\beta_T)_s \quad (15)$$

$$\rho_{eff} = (1 - \phi)\rho_f + \phi\rho_s \quad (16)$$

### III. RESULTS AND DISCUSSION

The solutions of the governing equations are obtained by Comsol Multiphysics finite element analysis and simulation software for Rayleigh numbers from  $10^5$  to  $10^7$ , for solid volume fractions of 8%. CuO was taken as nanoparticles and the ratio of the nanolayer thickness to the original particle radius was taken as a fixed value of 0.1. Water was used as the base fluid with  $Pr=6.2$ . The thermo-physical properties of the fluid and solid phase are shown in Table 1.  $err \leq 10^{-6}$  is selected as convergence criteria, where  $err$  is relative error based on the Euclidean norm:

$$err = \left[ \frac{1}{N} \sum_{i=1}^N \left( \frac{|E_i|}{W_i} \right)^2 \right]^{1/2}, \quad W_i = \max(|U_i|, S_i) \quad (17)$$

where N is the number of degrees of freedom,  $E_i$  is the error and  $U_i$  is the dependent variable and S is the scale factor.

TABLE I  
THERMOPHYSICAL PROPERTIES OF BASE FLUID AND NANOPARTICLE

Property	Water	CuO
$\rho$ (kg/m <sup>3</sup> )	997.1	6500
$C_p$ (J/kgK)	4179	535.6
k (W/mK)	0.613	20
$\alpha \times 10^7$ (m <sup>2</sup> /s)	1.47	57.45
$\beta_T \times 10^6$ (1/K)	210	51

The effect of Rayleigh number and nanoparticle usage on the flow and heat transfer in the electronic control unit can be seen in Figures 2-7. As can be observed from the figures, the fluid particles move upward along the inner cylinders due to the bouncy forces as a result of uniform heat flux on their surfaces. The hot fluid particles rise along the inner cylinders until they reach near the top surface where they turn towards the surface of the outer cylinder and the separation wall. Then they turn downward near those walls. Finally, the restriction imposed by the bottom wall forces the fluid particles to turn towards the hot walls. The flow paths are completed as the colder fluid particles are entrained to the ascending flows. The other half of the outer cylinder where there are no inner cylinders, the separation wall serves as a heater. Therefore, the fluid particles move upwards by the effect of bouncy forces along this separation wall. Then, the fluid particles move toward the surface of the outer cylinder because of the restriction imposed by the top wall. Followed by, the fluid particles move downwards as they are cooled. Then, the fluid particles move toward the surface of the separation wall because of the restriction imposed by the bottom wall. At lower Ra numbers, circulation intensity is weaker in the region with inner cylinders compared to the region with no inner cylinders due to the higher viscous forces and weak buoyancy forces. However, when the Rayleigh number increases, circulation becomes stronger in this region as the buoyancy forces become dominant. As can be seen in the figures, as the Rayleigh number increases, the temperature of the electronic control module decreases as a result of stronger circulation. The nanoparticle usage increases energy transport from heated surfaces to the nearby fluid because of the increase of its thermal conductivity coefficient. This creates a positive effect on the circulation intensity. The nanoparticle usage also increases fluid viscosity, as seen from Eq. (13). This leads to an increase at viscous forces. Because this effect is stronger than the effect caused by thermal conductivity increase, a decrease is seen in the circulation intensity due to the usage of nanoparticles in the base fluid. As stated before, nanoparticle usage increases the thermal conductivity coefficient of the fluid significantly. Consequently, even though nanoparticle usage decreases the circulation intensity, an increase is seen in

the heat transfer and therefore a decrease in the temperatures inside the electronic control unit.

#### ACKNOWLEDGMENT

The authors acknowledge the financial support received from Trakya University Scientific Research Project Unit.

#### REFERENCES

- [1] J. A. Eastman, S. U. S. Choi, W. Yu, and L. J. Thompson, "Anomalously increased effective thermal conductivity of ethylene glycol-based nanofluids containing copper nanoparticles," *Applied Physical Letters*, vol. 78, pp. 718–720, 2001.
- [2] S. U. S. Choi, Z. G. Zhang, W. Yu, F. E. Lockwood, and E. A. Grulke, "Anomalous thermal conductivity enhancement in nanotube suspension," *Applied Physical Letters*, vol. 79, pp. 2252–2254, 2001.
- [3] Y. Xuan, and Q. Li, "Heat transfer enhancement of nanofluids," *Int. J. Heat Fluid Flow*, vol. 21, pp. 58–64, 2000.
- [4] P. Keblinski, S. R. Phillpot, S. U. S. Choi, and J. A. Eastman, "Mechanisms of heat flow in suspensions of nano-sized particles nanofluids," *Int. J. Heat Mass Transfer*, vol. 45, pp. 855–863, 2002.
- [5] W. Yu, and S. U. S. Choi, "The role of interfacial layers in the enhanced thermal conductivity of nanofluids: A renovated Maxwell model," *J. Nanoparticle Research*, vol. 5, pp. 167–171, 2003.
- [6] Y. Xuan, Q. Li, Y. Xuan, and Q. Li, "Experimental Research on the Viscosity of Nanofluids," Report of Nanjing University of Science and Technology, 1999.

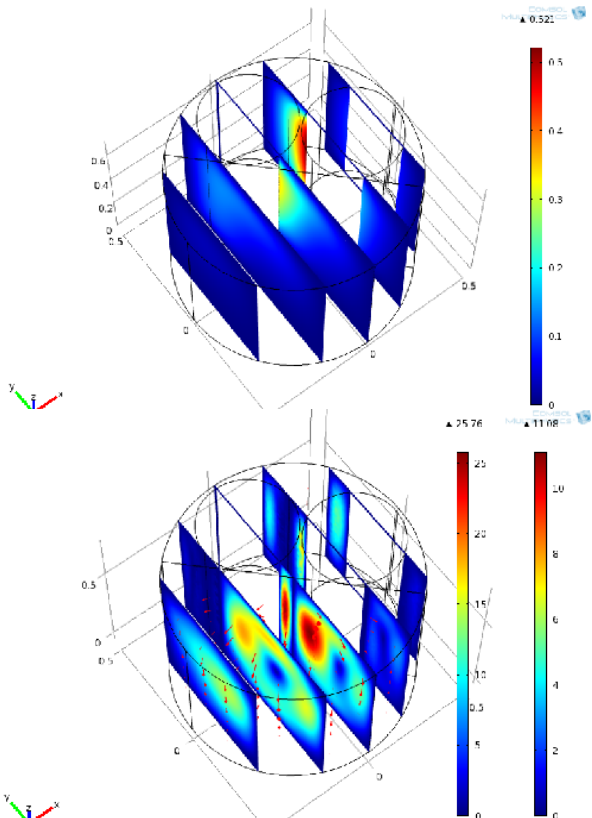


Fig. 2 Temperature and velocity fields for  $Ra=10^5$ ,  $\phi=0\%$

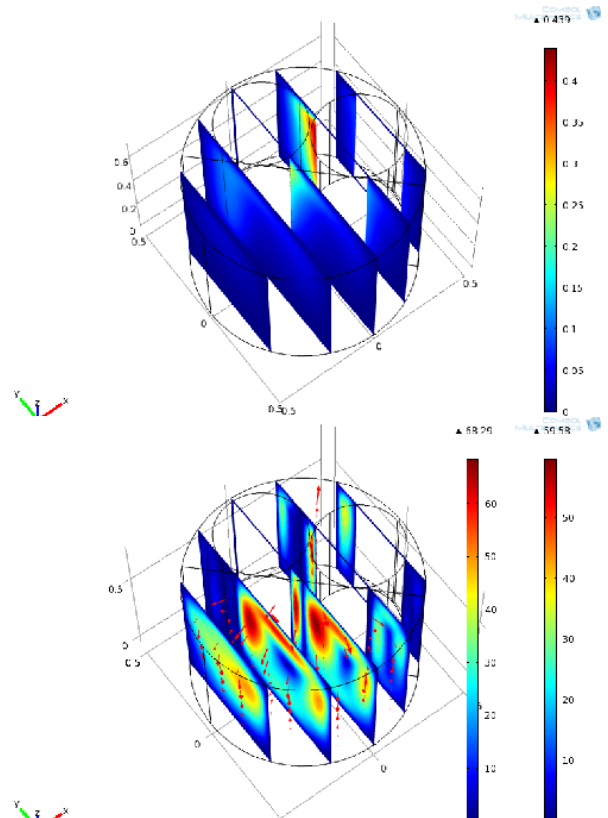


Fig. 4 Temperature and velocity fields for  $Ra=10^5$ ,  $\phi=0\%$

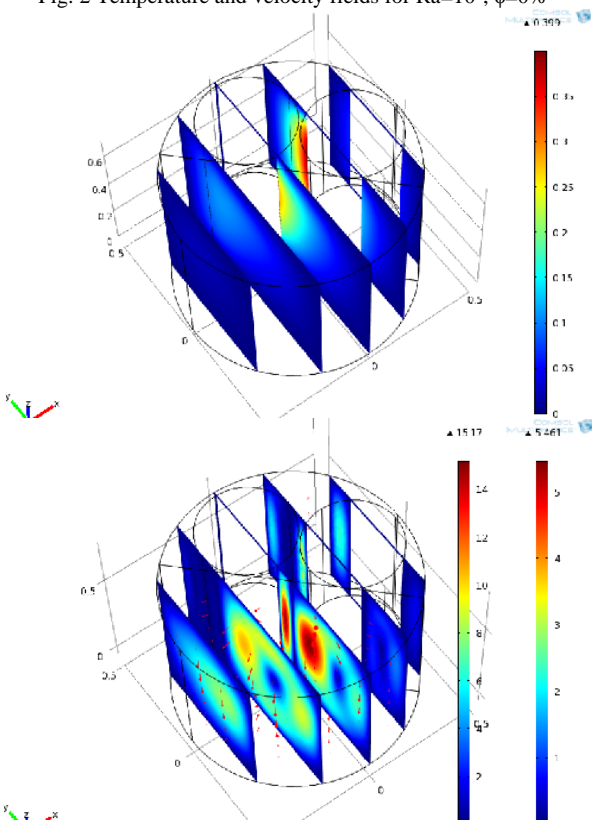


Fig. 3 Temperature and velocity fields for  $Ra=10^5$ ,  $\phi=8\%$

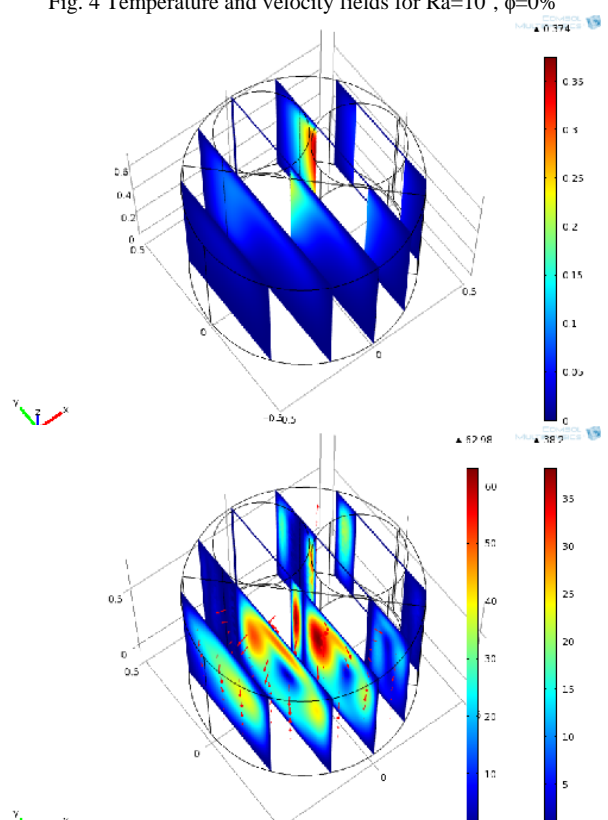


Fig. 5 Temperature and velocity fields for  $Ra=10^5$ ,  $\phi=8\%$

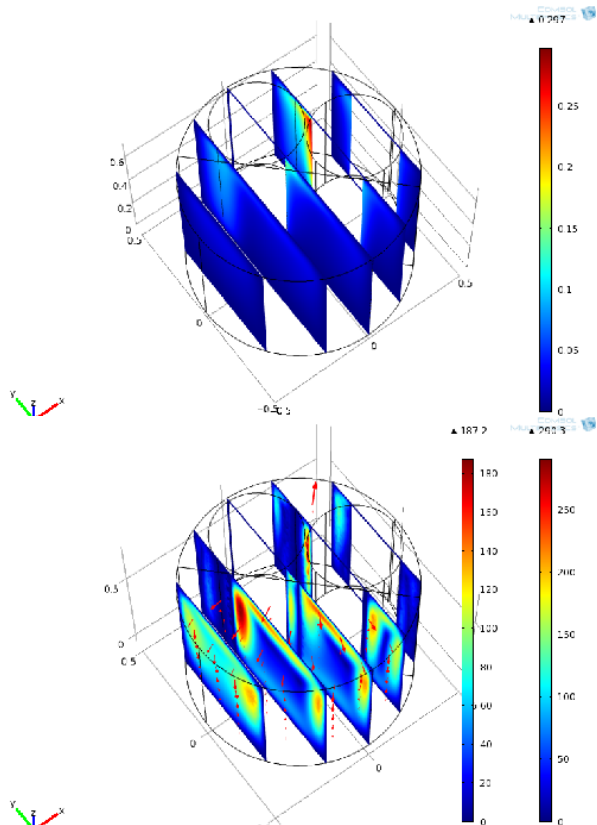


Fig. 6 Temperature and velocity fields for  $Ra=10^7$ ,  $\phi=0\%$

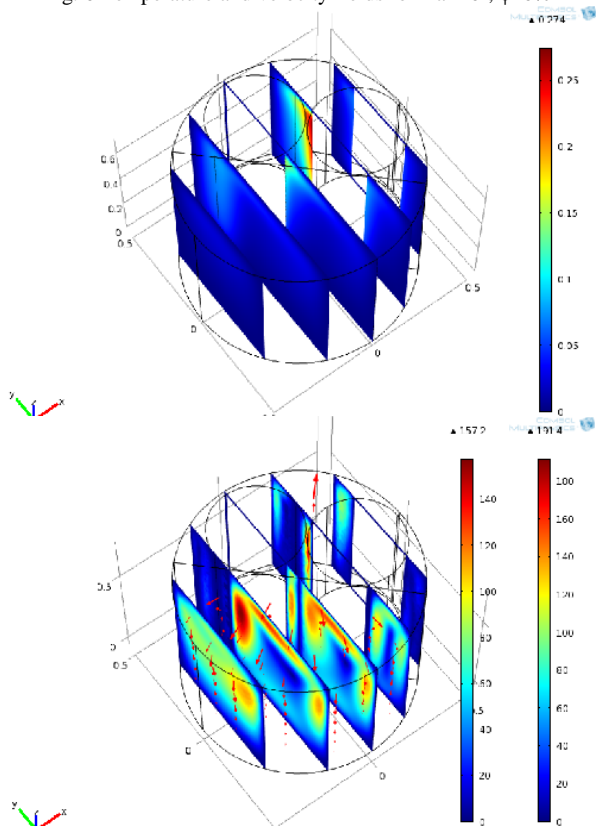


Fig. 7 Temperature and velocity fields for  $Ra=10^7$ ,  $\phi=8\%$